Bioorganic & Medicinal Chemistry 20 (2012) 750–758

Contents lists available at SciVerse ScienceDirect

Bioorganic & Medicinal Chemistry

journal homepage: www.elsevier.com/locate/bmc

STAT6 phosphorylation inhibitors block eotaxin-3 secretion in bronchial epithelial cells

Li Zhou [a], Tomohiko Kawate [a], Xiaorong Liu [a], Young Bae Kim [a], Yajuan Zhao [a], Guohong Feng [a], Julian Banerji [a], Huw Nash [b], Charles Whitehurst [b], Satish Jindal [b], Arshad Siddiqui [b], Brian Seed [a,*], Jia L. Wolfe [a]

[a] Center for Computational and Integrative Biology, Massachusetts General Hospital, 185 Cambridge St., Boston, MA 02114, USA
[b] Neogenesis, Cambridge, MA 02139, USA

ARTICLE INFO

Article history:
Received 30 September 2011
Revised 28 November 2011
Accepted 3 December 2011
Available online 17 December 2011

Keywords:
Signal transducers and activators of transcription 6
Allergic inflammatory disease
STAT6 binder
STAT6 inhibitor
Eotaxin-3

ABSTRACT

The STAT6 (signal transducer and activator of transcription 6) protein facilitates T-helper cell 2 (Th2) mediated responses that control IgE-mediated atopic diseases such as asthma. We have identified compounds that bind to STAT6 and inhibit STAT6 tyrosine phosphorylation induced by IL-4. In the bronchial epithelial cell line BEAS-2B, compound (***R***)-**84** inhibits the secretion of eotaxin-3, a chemokine eliciting eosinophil infiltration. (***R***)-**84** appears to prevent STAT6 from assuming the active dimer configuration by directly binding the protein and inhibiting tyrosine phosphorylation.

1. Introduction

With an estimated prevalence of 100 million affected individuals worldwide, asthma is among the most common of chronic diseases in developed world populations. The etiology of asthma is complex, but a broad consensus holds that airway exposure to allergens results in activation of antigen-specific Th2 cell development and the secretion of Th2 cytokines such as IL-4 and IL-13, which are critical regulators of inflammatory responses.[1,2] The airways of asthmatics are characterized by airway hyperreactivity (AHR, defined by exaggerated airflow obstruction in response to bronchoconstrictors), mucus overproduction, and chronic eosinophilic inflammation, all of which have been inferred to be mediated by STAT6-dependent pathways. Genetic deletion of STAT6 in mice broadly blunts Th2 axis responsiveness, and yields phenotypic evidence that STAT6 is a central downstream mediator for airway reactivity.[3,4] Targeted expression of STAT6 in epithelial cells is sufficient for IL-13 induced AHR and mucus production.[5] Because STAT6-null mice are healthy under laboratory conditions, STAT6 has been considered a promising target for the treatment of asthmatic disease in humans.

Like other members of the STAT family, STAT6 has a dual role as signaling molecule and transcription factor. Activation of STAT6 is initiated by binding of cytokines IL-4 and IL-13 to their cognate receptors, which leads to the activation of Janus tyrosine kinases (JAKs) including JAK1, JAK2, JAK3, and Tyk2, which are associated with the cytoplasmic tails of the receptors.[6] The activated JAKs phosphorylate receptor tyrosine residues, generating a docking site for cytoplasmic STAT6. Following binding to the receptor phosphotyrosines by its SH2 domain, STAT6 becomes phosphorylated at conserved tyrosine residue Y641 and undergoes dimerization mediated by phosphotyrosine–SH2 interaction. The activated STAT6 dimers translocate rapidly to the nucleus, where they induce gene expression.

STAT proteins were originally thought to adopt a monomeric state prior to activation.[7] However, recent evidence suggests the existence of an alternate inactive dimer state in which the transcription factor resides prior to activation.[8,9] The conformation of this dimer is antiparallel in the case of STAT1.[10,11] After tyrosine phosphorylation, the antiparallel dimers are transformed into a parallel configuration, which is established by mutual phosphotyrosine–SH2 interactions. In STAT1 this conformation change results in a 200-fold increase in DNA binding activity.[12] If STAT6 were to undergo similar conformational changes they would take place upon phosphorylation at Y641.

* Corresponding author. Tel.: +1 617 726 5975; fax: +1 617 643 3328.
E-mail address: bseed@ccib.mgh.harvard.edu (B. Seed).

0968-0896/$ - see front matter © 2011 Elsevier Ltd. All rights reserved.
doi:10.1016/j.bmc.2011.12.006

Because STAT proteins control fundamental processes in the hematopoietic system and beyond, there is a growing interest in discovering small molecule inhibitors of their action. To accomplish this, cell-based screening strategies have been widely utilized to identify and evaluate compounds that can inhibit one or more key steps involved in STAT activation, including recruitment to cytokine receptors, phosphorylation, dimerization, and DNA binding. Additional efforts have been devoted to the design and/or screening for inhibitors that can specifically inhibit key steps involved in STAT activation. For example, inhibitors that target the STAT SH2 domain,[13–16] STAT nuclear translocation,[17] and dimerization of phosphorylated STAT (using dominant-negative STAT peptides)[18] have been reported. Notably only very few STAT6 inhibitors have been disclosed to date,[18–22] and most of them have been identified through IL-4 or STAT6 reporter-based screening.[20–22] The mechanisms by which these STAT6 inhibitors act has yet to be established. Since cell-based reporter assays are not designed to distinguish STAT6-specific inhibition from that caused by the inhibition of a variety of upstream factors including cytokines, cytokine receptors, and JAKs, such screens may not select inhibitors that are specifically targeted to STAT6.

To discover specific STAT6 inhibitors, an affinity selection-mass spectrometry (AS-MS) method[23–25] was applied to identify small molecules that bind to recombinant human STAT6 specifically. Briefly, mass-encoded libraries of small molecule compounds were exposed to purified target protein. The target with any bound molecules was rapidly separated from free compounds by size exclusion chromatography, and the bound compounds were identified by LC/MS/MS. Following confirmation of hits by re-synthesis individual candidates were advanced for further characterization. The selected binders were further analyzed by cell-based reporter assays. A lead compound, (***R***)-**76**, was identified. Both (***R***)-**76** and its analog (***R***)-**84** demonstrated sub μM affinity for recombinant STAT6 by surface plasmon resonance (SPR) analysis. Both compounds inhibit STAT6-dependent signaling events in a reporter-based assay and block eotaxin-3 secretion by bronchial epithelial cells. STAT6 tyrosine phosphorylation is inhibited by these compounds, which may prevent the formation of STAT6 dimer in the active parallel configuration.

2. Results and discussion

2.1. Synthesis of (*R*)-76 and (*R*)-84

Compounds (***R***)-**76** and (***R***)-**84** were synthesized following the procedures outlined in Scheme 1. Suzuki coupling between 4-bromopyridine-2,6-dicarboxyl methyl ester and the boronic acid of benzothiophene and that of *N*-methyl-indole, respectively gave dicarboxylic esters that were hydrolyzed and condensed with aminoethyl-pyridine and (*R*)-3-methyl-2-butylamine in the presence of HOBt/EDCI catalyst to afford (***R***)-**76** and (***R***)-**84**, respectively. The condensation reactions may be carried out in a step-wise fashion, as indicated for the preparation of (***R***)-**76**, or in a one-pot process, as exemplified by the preparation of (***R***)-**84**.

2.2. Inhibition of STAT6 signaling

Recombinant human STAT6 was prepared following baculoviral infection of insect cells. The protein was screened against approximately 10 million compounds using Affinity Selection-Mass Spectrometry screening[23–25] to identify compounds that specifically bind to STAT6 protein. A number of compounds were selected and further tested for their ability to inhibit STAT6 signaling in a cell-based assay using a STAT6 reporter created by inserting six copies of an IL-4 responsive element in front of the *Photinus pyralis* luciferase gene.[26] The assay was designed to measure the degree of transcriptional activation of STAT6 stimulated by IL-4, and the effect of the compounds on such transcriptional activation. After co-transfection of the reporter construct and an expression vector encoding human STAT6, we detected a 30-fold increase in luciferase activity following exposure to IL-4 for 6 h (Fig. 2A). The induction was inhibited in the presence of a particular chemotype represented by compound (***R***)-**76** (Figs. 1 and 2A). *Renilla reniformis* luciferase under the control of the *Herpes simplex* thymidine kinase promoter was used as a control for transfection efficiency and cellular toxicity. The *Renilla* luciferase activity was only slightly affected by the compounds (data not shown), indicating that the inhibition of STAT6 reporter was not due to some general toxic effect. The compounds did not affect *Photinus* luciferase activity per se, as similar inhibition was observed when we used *Renilla* luciferase in place of *Photinus* luciferase as the reporter (data not shown). Based on the chemical structure of (***R***)-**76**, we designed and synthesized a series of analogs and tested them in the reporter assay. Among them compound (***R***)-**84** was selected for further analysis (Fig. 1). The IC_{50} values of the original lead compound (***R***)-**76** and the modified compound (***R***)-**84** are 3.2 μM and 2.7 μM, respectively. Mouse STAT6 is inhibited with similar IC_{50} values by these compounds (data not shown). For comparison we have included data for oxime **7Z** (shown in Fig. 1), a previously described STAT6 inhibitor,[27] as a reference.

2.3. Inhibition of eotaxin-3 secretion

Eotaxins are important mediators of eosinophil recruitment and activation in asthma. IL-4, IL-13 and TNF-α can induce secretion of eotaxin-3,[28] and eotaxin-3 secretion induced by IL-4 and IL-13 is mediated by STAT6.[29–32] To test if (***R***)-**76** and (***R***)-**84** can block secretion elicited by these agents, we carried out an eotaxin secretion assay using the bronchial epithelium cell line BEAS-2B. In this line IL-4 treatment induces eotaxin-3 secretion to >1 ng/ml after 24 h of cytokine exposure (Fig. 2B). Prolonging incubation time to 48 h increases accumulation to 2 ng/ml (Fig. 2C). BEAS-2B is more sensitive than the A549 cell line for this induction (Fig. 2B). (***R***)-**84** was able to suppress eotaxoin-3 secretion at 10 μM whereas **7Z** and (***R***)-**76** were not particularly effective (Fig. 2D). The IC_{50} for (***R***)-**84** was determined to be 2.74 μM, which is similar to that determined by the reporter assay. Although (***R***)-**76** and (***R***)-**84** bind equally well to STAT6 protein (see below), and (***R***)-**76** shows similar activity in the reporter assay, (***R***)-**76** is not as effective in the eotaxin-3 secretion assay. Figure 2E shows that eotaxin-3 secretion is inducible by IL-4 and/or IL-13, and that induction is further augmented when TNF-α is co-applied. At 10 μM concentration, (***R***)-**84** is able to suppress induction effectively (Fig. 2E).

2.4. (*R*)-76 and (*R*)-84 directly inhibit tyrosine phosphorylation of STAT6 without interfering with the interaction between STAT6 and phospho-IL-4Rα

STAT6 tyrosine phosphorylation by activated JAK kinases is a key step in STAT6 activation. In vivo this process involves the docking of STAT6 onto the cytoplasmic tail of phosphorylated IL-4Rα mediated through specific interactions between the SH2 domain of STAT6 and phosphorylated tyrosine residues on IL-4Rα. Since STAT6 binding to IL-4Rα is necessary for STAT6 phosphorylation, (***R***)-**76** or (***R***)-**84** could potentially inhibit STAT6 activation by blocking receptor binding. To investigate this possibility, we examined the interaction between STAT6 and an IL-4Rα-derived peptide representing the docking site. In an ELISA format, immobilized IL-4R peptide and its phosphorylated counterpart p-IL-4R peptide were tested for STAT6 recognition. As shown in Figure 3B, STAT6 binds to the phosphorylated p-IL-4R peptide with an EC_{50}

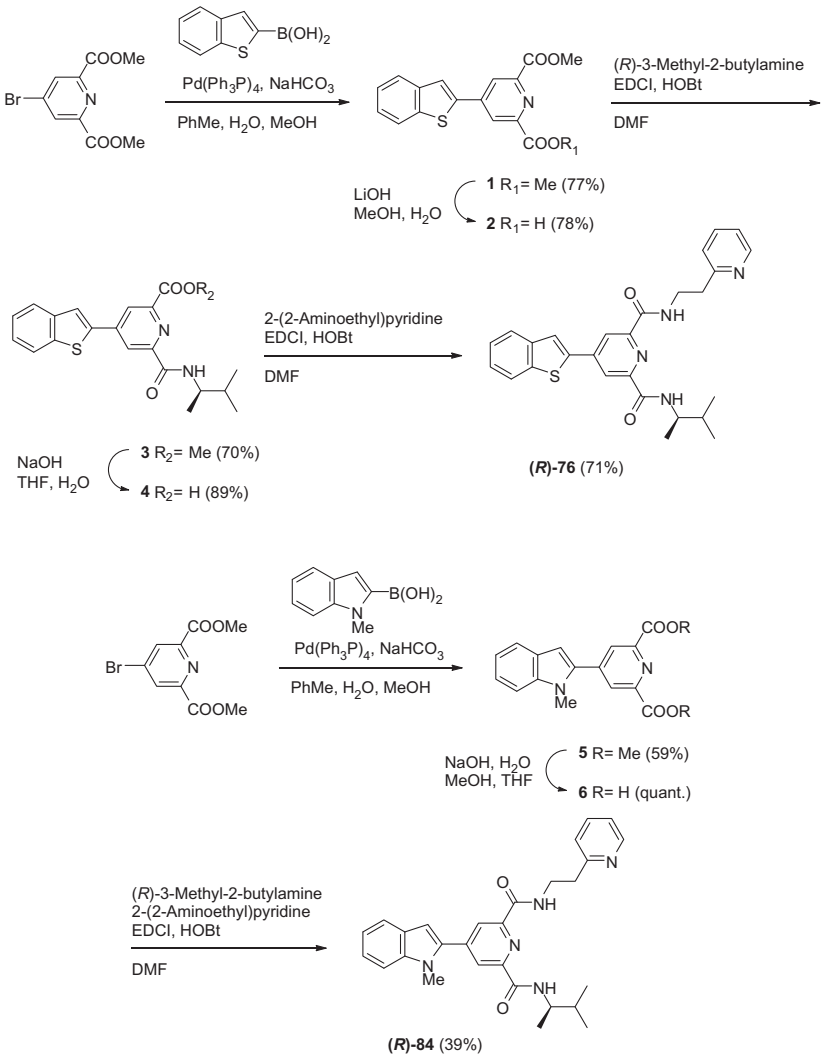

Scheme 1. Synthesis of compounds (***R***)-**76** and (***R***)-**84**.

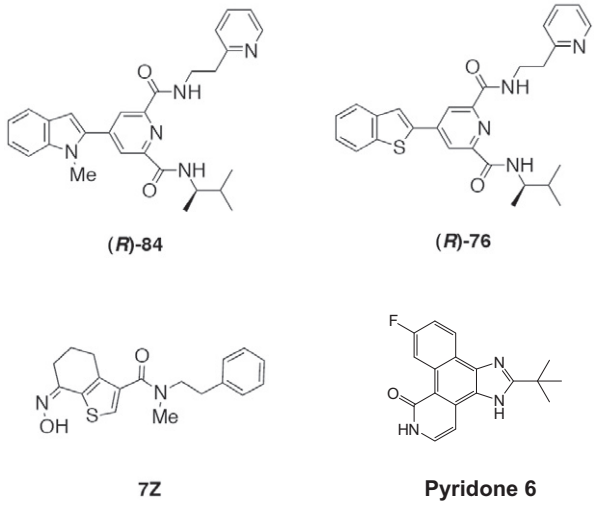

Figure 1. Compounds used in this study.

(132 nM) similar to that reported in the literature.[7] The interaction is not affected by any of the STAT6 inhibitors (Fig. 3C). This result suggests that these compounds do not interfere with the interaction between IL-4Rα and the SH2 domain of STAT6.

We next tested if STAT6 tyrosine phosphorylation is inhibited. In 293-EBNA cells transfected with human STAT6, IL-4 treatment causes STAT6 to undergo tyrosine phosphorylation and the phosphorylated STAT6 can be detected with an anti-phospho-tyrosine antibody (Fig. 3A). Because the induction occurs within minutes of IL-4 addition, the inhibitory effects of the compounds were tested by pre-incubating cells with different compounds at 10 μM for 1 h prior to IL-4 induction. After the addition of IL-4, the cells were further incubated for 6 h, harvested, lysed and subjected to immunoblot analysis. As shown in Figure 3A, (***R***)-**76** and (***R***)-**84** inhibited STAT6 phosphorylation, whereas **7Z** did not. This indicates that the inhibition of STAT6 signaling by **7Z** is via a different mechanism than that of (***R***)-**76** and (***R***)-**84**.

Because JAK kinases are responsible for IL-4/IL-13 induced STAT6 phosphorylation, and JAK2 is commonly involved in the STAT6 activation,[33] we next tested if (***R***)-**76** and (***R***)-**84** could inhibit JAK2 kinase activity. Figure 3D illustrates that neither (***R***)-**76** and (***R***)-**84** inhibited JAK2 up to 10 μM, whereas Pyridone 6, a known JAK2 inhibitor, inhibited activity in a dose-dependent manner. We conclude from these results that (***R***)-**76** and (***R***)-**84** specifically inhibit STAT6 tyrosine phosphorylation primarily by directly interacting with STAT6.

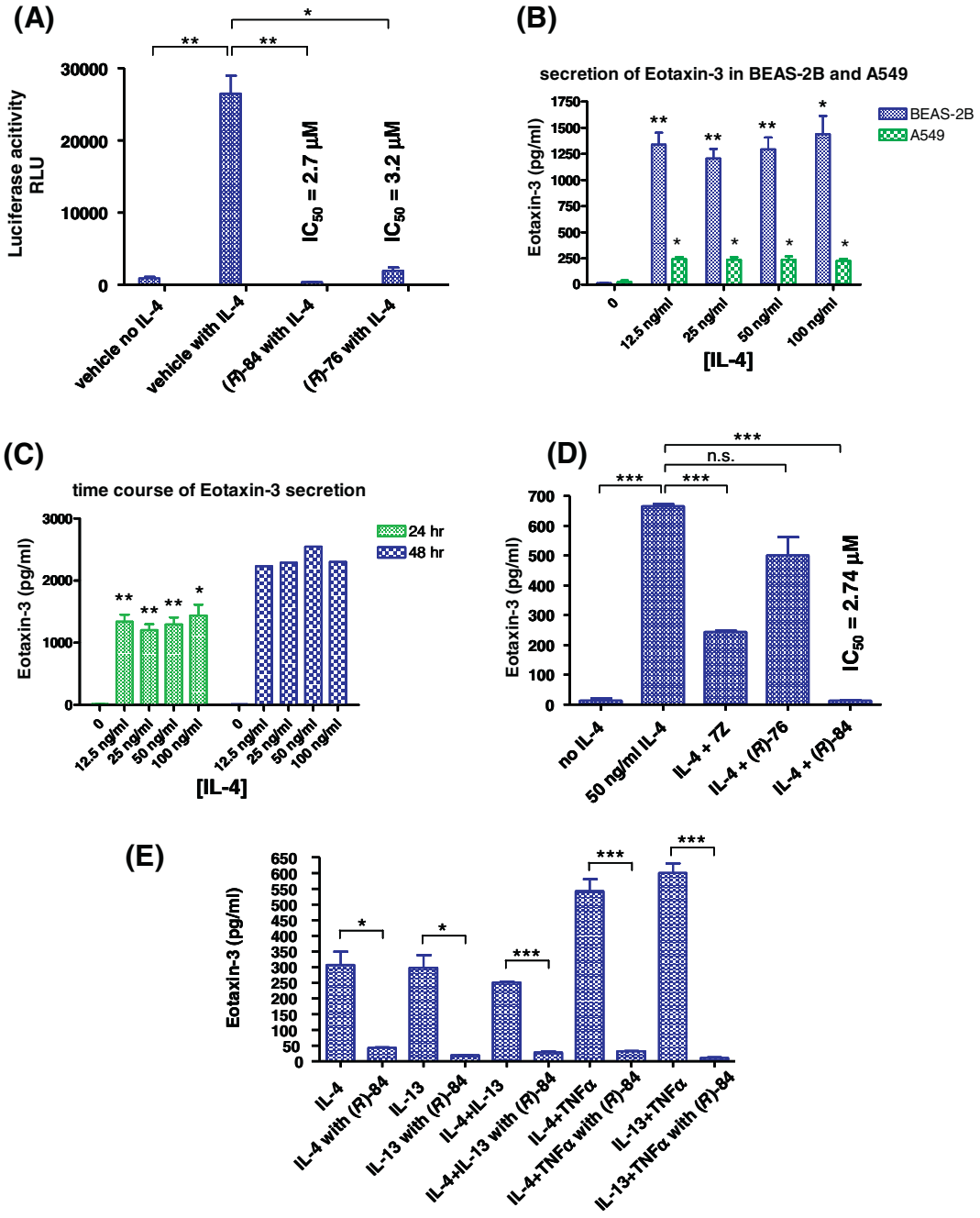

Figure 2. Inhibition of STAT6 signaling in cell-based assays. (A) Induction of STAT6 reporter luciferase activity by IL-4 (10 ng/ml) in 293-EBNA cells, and inhibition by (***R***)-**84** or (***R***)-**76** at 10 μM. (B) Eotaxin-3 secretion in BEAS-2B and A549 cells after induction with various concentrations of IL-4 for 24 h. (C) Eotaxin-3 secretion in the BEAS-2B cell line after IL-4 induction for 24 h and 48 h. (D) Inhibition of eotaxin-3 secretion by **7Z**, (***R***)-**76**, or (***R***)-**84** at 10 μM after 24 h IL-4 induction. (E) Secretion of eotaxin-3 induced by IL-4 and IL-13, alone or in combination with TNF-α, and inhibition of each induction by (***R***)-**84** at 10 μM. Error bars are sd; $^{*}P$ <0.05, $^{**}P$ <0.01, $^{***}P$ <0.001, ns, not significant, in two-tailed *t*-test.

2.5. SPR analysis of STAT6–inhibitor interactions

To characterize the interactions between STAT6 and the inhibitors, surface plasmon resonance (SPR) technology was applied. Recombinant STAT6 was immobilized to a BIAcore Series S Sensor Chip CM5 by direct conjugation (amide formation) using an amine coupling kit. Each analyte, (***R***)-**76**, (***R***)-**84**, or **7Z**, was injected in the mobile phase, and the binding of each compound to surface-bound STAT6 was detected as a change of SPR response measured in resonance units (RU). The resulting SPR sensorgrams corresponding to complex formation and dissociation were recorded (Fig. 4), from which kinetic association rate (k_a) and dissociation rate (k_d) constants were derived by global fitting of data to 1:1 Langmuir binding model. Based on the k_d and k_a values, the equilibrium dissociation constant ($K_D = k_d/k_a$) can be calculated. As summarized in Table 1, (***R***)-**76** and (***R***)-**84** exhibited very similar binding kinetics and binding affinity to STAT6, whereas **7Z** showed a slower dissociation rate and a significantly slower association rate than others, resulting in a much weaker binding affinity.

It is also notable that the binding constants observed for compounds (***R***)-**76** and (***R***)-**84** are similar to the IC_{50} values they exhibited in STAT6 reporter assays (Fig. 2D). This correlation suggests that direct STAT6 binding may be the major contributing factor to the inhibition of STAT6 activity in the cell based assays.

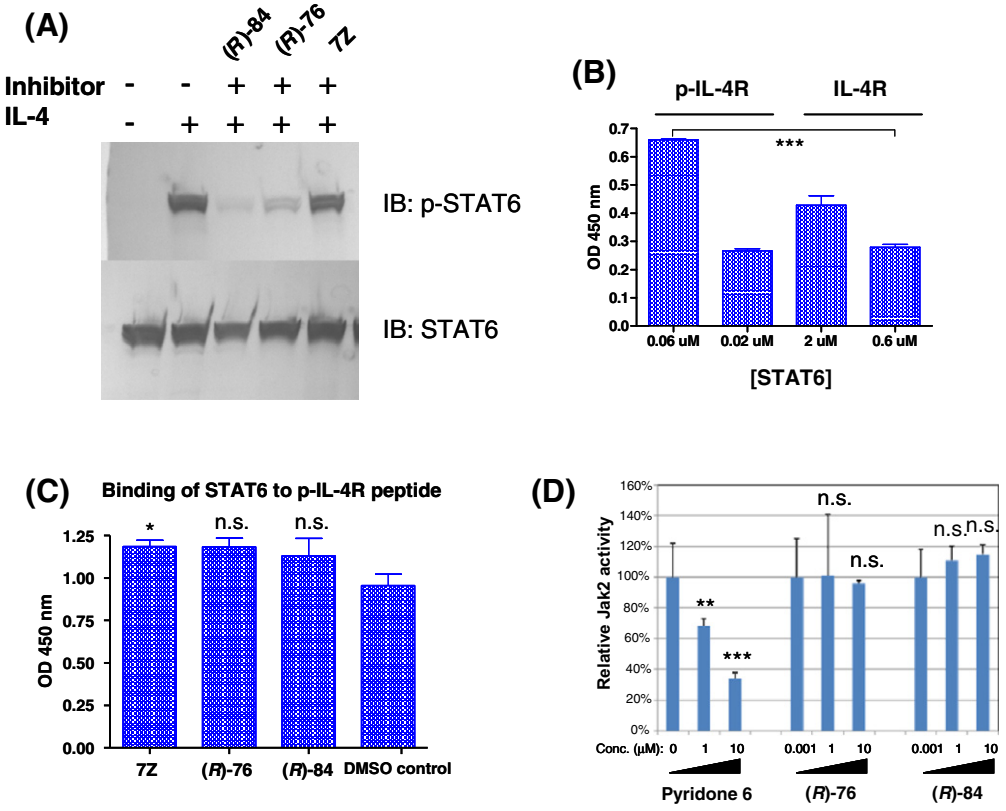

Figure 3. Effect of STAT6 signaling inhibitors on individual activation steps. (A) (***R***)-**84** or (***R***)-**76** inhibits IL-4 induced STAT6 phosphorylation as analyzed by western blot. (B) Interactions between STAT6 and immobilized IL-4R derived peptides analyzed by ELISA. (C) Effect of STAT6 inhibitors on the STAT6/IL-4R interaction analyzed by ELISA. (D) Effect of (***R***)-**76**, (***R***)-**84**, and known JAK2 inhibitor Pyridone 6 on JAK2 kinase activity. Error bars are sd; $^{*}P$ <0.05, $^{***}P$ <0.001, ns, not significant.

2.6. STAT6 adopts a dimeric form in the presence of the inhibitors

Many members in the STAT family, including STAT1, STAT3, STAT4, have been shown to form dimers in the non-phosphorylated state, in an antiparallel dimerization mediated by interactions at the N-terminus of the protein.[10,11] Upon tyrosine phosphorylation, the STAT dimers change to a parallel dimer structure stabilized by SH2 domain-phosphotyrosine interaction. Since STAT6 tyrosine phosphorylation is inhibited by (***R***)-**76** and (***R***)-**84**, we tested if these compounds would have any effect on STAT6 basal dimer formation. We constructed expression vectors encoding STAT6 with an HA tag or a myc tag and cotransfected them in equal proportion to allow the detection of randomly assorted heterodimers forming after translation. Immunoprecipitation by anti-HA agarose and blot detection with anti-myc antibody showed that no difference in abundance of heterodimers could be detected before or after IL-4 treatment (Fig. 5A). This result is in agreement with observations of resting state STAT dimers made elsewhere.[10,11] (***R***)-**76** and (***R***)-**84** did not affect the STAT6 dimer formation per se, but in their presence the dimer remained unphosphorylated in an inactive configuration even after IL-4 induction (Fig. 5B). Data presented in Figure 5 is also in agreement with the results described in Figure 3A that **7Z** does not inhibit STAT6 phosphorylation.

3. Discussion

In previously reported campaigns to identify STAT6 inhibitors, various strategies have been applied. These have included inhibition of SH2 domain interaction, inhibition of STAT6 and IL-4R interaction,[34] inhibition of STAT nuclear translocation,[17] and DNA binding inhibition. To date there has been no report of which we are aware in which full length recombinant STAT6 protein was used as the target for compound screening.

The STAT6 inhibitors described here implicate an interference site on STAT6 that involves tyrosine phosphorylation. The mechanism of action appears to involve inhibition of STAT6 activation, presumably by stabilization of the STAT6 dimer in an inactive configuration. Since structural studies on STAT dimers have established that they undergo conformational changes from an antiparallel to a parallel configuration, binding of (***R***)-**76** or (***R***)-**84** may have blocked such a conformational transition (Fig. 6). However it is also possible that the inhibitors promote the formation of an alternate dimer structure.

An SPR-based binding assay confirmed that both (***R***)-**76** and (***R***)-**84** directly interact with STAT6 with an affinity in the sub μM range. When tested in cell-based assays, the compounds showed IC_{50} values in the μM range. Replacing the benzothiophene moiety in (***R***)-**76** with *N*-methyl-indole in (***R***)-**84** markedly improved inhibition efficacy in various cell based assays, even though (***R***)-**76** and (***R***)-**84** appear to have similar binding affinity to STAT6 in vitro. While it is still unclear why (***R***)-**84** shows superior activity to (***R***)-**76** in STAT6 inhibition in cell based assay, it is possible, for example, that the molecules differ in their ability to obstruct other conformation-sensitive components of STAT6 signaling.

After the conclusion of the present study, a recent report described a non-agonist PPARγ ligand blocking Cdk5-mediated phosphorylation.[36] It is noteworthy that the mechanism of action bears some similarity to that proposed here, that is, the reported inhibitory effect is mediated through binding to a transcriptional factor, not to its kinase.

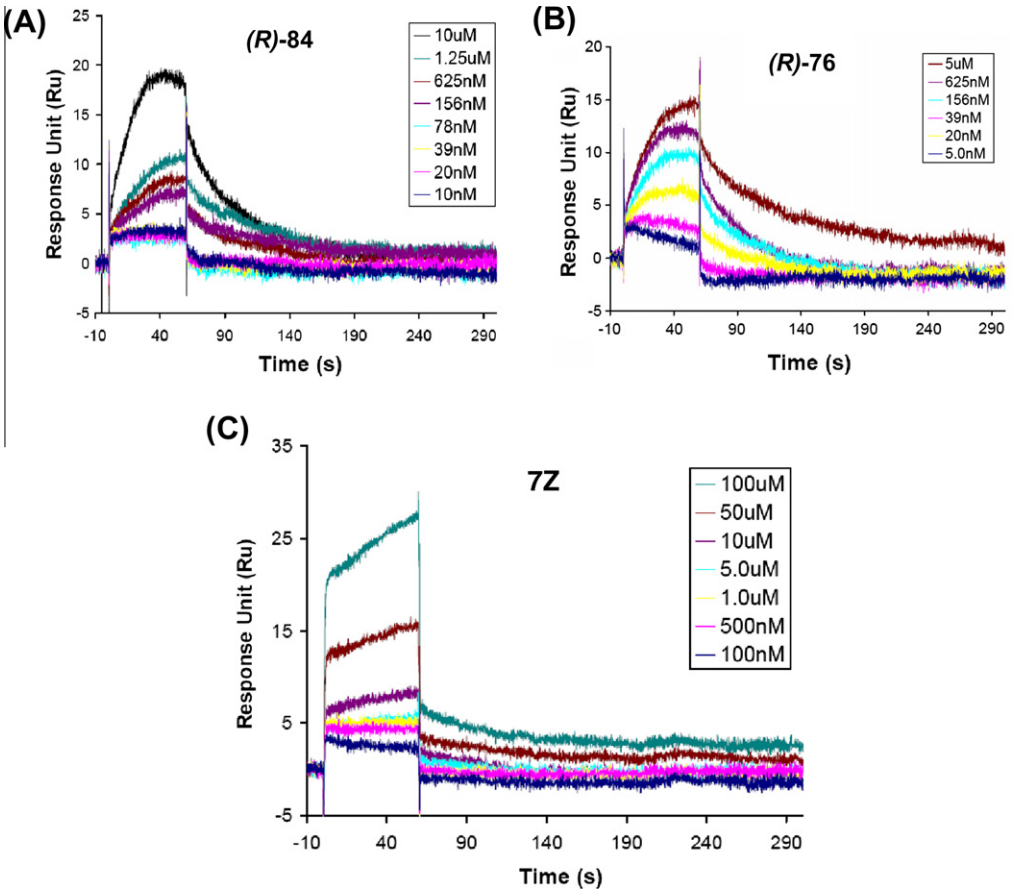

Figure 4. SPR sensorgrams of STAT6 binding by small molecule inhibitors (***R***)-**84**, (***R***)-**76**, and **7Z**.

Table 1
Equilibrium dissociation constant (K_D), association rate (k_a), and dissociation rate (k_d), and χ^2 value obtained by global fitting of SPR sensorgrams to a 1:1 Langmuir binding model

Inhibitor	k_a (1/Ms)	k_d (1/s)	K_D (μM)	χ^2
(***R***)-**84**	2.546×10^4	0.01669	0.6556	0.769
(***R***)-**76**	2.892×10^4	0.02028	0.7014	2.56
7Z	2.611×10	0.001931	73.97	0.775

We have demonstrated that (***R***)-**76** and (***R***)-**84** directly bind to STAT6 and inhibit STAT6 phosphorylation. To our knowledge this mode of STAT6 inhibition has not been previously reported. A tricyclic heptaketide (TMC-264) was found in an IL-4 reporter screen of microbial extracts, and the compound was reported both to affect STAT6 tyrosine phosphorylation and to be less potent against STAT1 phosphorylation.[22] A series of STAT6 inhibitors based on 4-[(3-methylphenyl)amino]pyrimidine derivatives were screened using IL-4R reporter assay, and their STAT6 binding status has not been described.[20,21] Compound **7Z** was also originally discovered by screening with a STAT6 reporter assay,[27] and we have shown here by SPR analysis that this inhibitor does not have mechanistically relevant affinity for STAT6, with an observed K_D at least 100-fold higher than that of (***R***)-**76** and (***R***)-**84**.

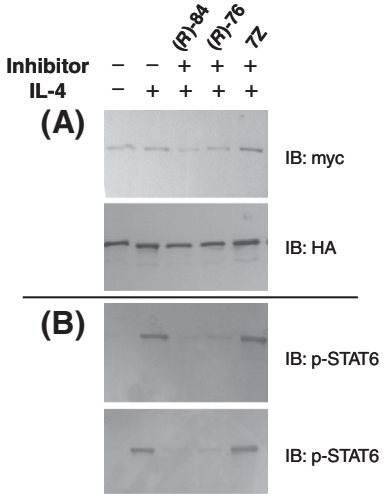

Figure 5. STAT6 heterodimerization can be detected prior to IL-4 induction and is not affected by inhibitors. (A) Immunoprecipitation (IP) with anti-HA followed by immunoblot (IB) with anti-myc and anti-HA. (B) Re-probed with anti-phospho-STAT antibody.

4. Experimental

4.1. Synthesis

NMR spectra were recorded on a Varian AS400 MHz Nuclear Magnetic Resonance Spectrometer with a multinuclear probe. Mass spectrometry analysis was performed on a Bruker Esquire 3000 plus LC/MS system using electrospray ionization method.

4.1.1. 4-(Benzo[*b*]thiophen-2-yl)pyridine-2,6-dicarboxylic acid dimethyl ester (1)

A mixture of 4-bromopyridine-2,6-dicarboxylic acid methyl ester (548 mg, 2.00 mmol), benzothiophene-2-boronic acid (401 mg,

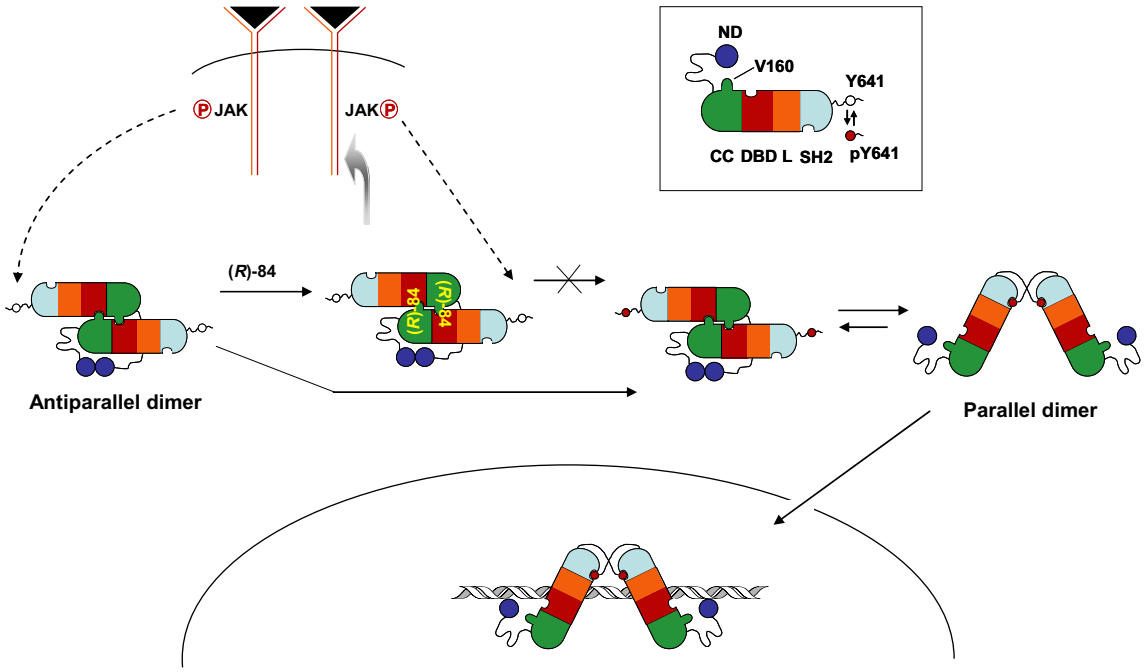

Figure 6. Schematic of STAT6 binding and inhibition by (***R***)-**84**. STAT6 domain structural features include,[35] N-terminus domain (ND), coiled:coil domain (CC), DNA-binding domain (DBD), linker domain (L), and SH2 domain (SH2). The tyrosine residue undergoes phosphorylation, Y641, is shown as a red dot after phosphorylation. V160 in the CC domain corresponds to a residue that has been shown important in the formation of antiparallel structure of STAT1.[35]

2.25 mmol), sodium bicarbonate (332 mg, 3.95 mmol), and tetrakis(triphenylphosphine)palladium (119 mg, 0.10 mmol) was placed in a 100 mL-flask and dried under vacuum for 2.5 h. In a separate flask, a mixture of toluene (20 mL), methanol (5 mL) and water (5 mL) was degassed by bubbling argon gas for 2.5 h, and added to the flask containing reagents. The resulting mixture was stirred under argon atmosphere at 70 °C for 2.5 h. The mixture was cooled to room temperature and evaporated to dryness. The residue was partitioned between dichloromethane and water, and the organic phase was collected, washed with brine and dried over sodium sulfate. After rotary evaporation, the residue was crystallized from ethyl acetate–hexanes to afford **1** (488 mg) as a white powder. Chromatography of the mother liquor on silica gel (10–60% ethyl acetate in hexanes) afforded an additional 19 mg of the product, providing 507 mg of **1** in total (77% yield). ^{1}H NMR (400 MHz, $CDCl_3$) δ 8.58 (s, 2H), 7.97 (s, 1H), 7.90 (m, 2H), 7.44 (m, 2H), 4.07 (s, 6H). ^{13}C NMR (101 MHz, $CDCl_3$) δ 165.20, 149.12, 144.62, 140.48, 140.08, 138.87, 126.39, 125.42, 124.88, 124.50, 124.09, 122.76, 53.56.

4.1.2. 4-(Benzo[*b*]thiophen-2-yl)-6-(methoxycarbonyl) picolinic acid (2)

To a mixture of dimethyl ester **1** (172 mg, 0.53 mmol) in methanol (50 mL) and tetrahydrofuran (20 mL) was added 1 N aqueous sodium hydroxide (0.55 mL, 0.55 mmol) and the resulting mixture was stirred at room temperature for 28 h. The reaction was quenched with 1 N aqueous hydrochloric acid (0.6 mL) and evaporated to dryness. The residue was suspended with dichloromethane–methanol (v/v, 1:1) and filtered through a pad of diatomaceous earth. The filtrate was evaporated and partitioned between dichloromethane and water. The organic phase was collected and dried over sodium sulfate. Evaporation of the solvents afforded compound **2** (128 mg, 78% yield) as an orange solid, which was used in next step without further purification. ^{1}H NMR (400 MHz, DMSO-d_6) δ 13.74 (br s, 1H), 8.48 (m, 3H), 8.07 (m, 1H), 7.94 (m, 1H), 7.46 (m, 2H), 3.95 (s, 3H).

4.1.3. (*R*)-4-(Benzo[*b*]thiophen-2-yl)-6-(3-methyl-butan-2-ylcarbamoyl)picolinic acid methyl ester (3)

To a mixture of compound **2** (127 mg, 0.41 mmol) and 1-hydroxybenzotriazole (HOBt, 99 mg, 0.73 mmol) in *N*,*N*-dimethylformamide (DMF, 3 mL) was added 1-ethyl-3-dimethyl-aminopropylcarbodiimide hydrochloride (EDCI, 123 mg, 0.64 mmol). The mixture was stirred at room temperature for 15 min. A solution of (*R*)-3-methyl-2-butylamine (41 mg, 0.47 mmol) in DMF (2 mL) was added and the resulting mixture was stirred at room temperature for 16 h. The mixture was diluted with dichloromethane, washed with water, brine, and dried over sodium sulfate. Evaporation of the solvents afforded a residue, which was chromatographed on a silica gel (ethyl acetate–hexanes) to provide ester amide **3** (109 mg, 70% yield). ^{1}H NMR (400 MHz, $CDCl_3$) δ 8.67 (d, J = 1.60 Hz, 1H), 8.47 (d, J = 1.60 Hz, 1H), 8.05 (br d, J = 9.20 Hz, 1H), 7.96 (s, 1H), 7.88 (m, 2H), 7.42 (m, 2H), 4.11 (m, 1H), 4.06 (s, 3H), 1.88 (m, 1H), 1.26 (d, J = 6.80 Hz, 3H), 1.01 (d, J = 6.80 Hz, 3H), 1.00 (d, J = 6.40 Hz, 3H).

4.1.4. (*R*)-4-(Benzo[*b*]thiophen-2-yl)-6-(3-methylbutan-2-yl-carbamoyl)picolinic acid (4)

To a solution of ester amide **3** (98 mg, 0.26 mmol) in tetrahydrofuran (4 mL) was added 1 N aqueous sodium hydroxide (0.5 mL, 0.5 mmol) and the mixture was stirred at room temperature. After 13 h, the reaction was quenched by 1 N aqueous hydrochloric acid (0.5 mL) and evaporated to dryness. The residue was partitioned between dichloromethane and half saturated brine. The organic phase was collected and dried over sodium sulfate. Evaporation of the solvents gave acid **4** (84 mg, 89% yield), which was used in the next step without further purification. ^{1}H NMR (400 MHz, DMSO-d_6) δ 13.30 (br s, 1H), 8.87 (d, J = 8.80 Hz, 1H), 8.49 (m, 3H), 8.07 (m, 1H), 7.93 (m, 1H), 7.45 (m, 2H), 3.90 (m, 1H), 1.81 (m, 1H), 1.18 (d, J = 6.80 Hz, 3H), 0.92 (d, J = 7.20 Hz, 3H), 0.90 (d, J = 7.20 Hz, 3H). ESI-MS: m/z $[M+Na]^+$ 391.1, $[M+H]^+$ 369.2, $[M-H]^-$ 367.0.

4.1.5. (*R*)-4-(Benzo[*b*]thiophen-2-yl)-N^2-(3-methylbutan-2-yl)-N^6-(2-(pyridin-2-yl)ethyl)pyridine-2,6-dicarboxamide ((*R*)-76)

A mixture of compound **4** (79 mg, 0.21 mmol), 1-hydroxybenzotriazole (HOBt, 46 mg, 0.34 mmol) and 1-ethyl-3-dimethylaminopropylcarbodiimide hydrochloride (EDCI, 67 mg, 0.35 mmol) in DMF (4 mL) was stirred at room temperature for 2 h. In a separate flask, 2-(2-aminoethyl)pyridine (24 mg, 0.20 mmol) was dissolved in DMF (1 mL), to which 2 mL of the compound **4** solution prepared above was added. After stirring at room temperature for 16 h, the mixture was evaporated to dryness. The residue was dissolved in dichloromethane, washed with water, brine, and dried over sodium sulfate. Evaporation of the solvent afforded a residue, which was chromatographed on silica gel (ethyl acetate–hexanes) to provide diamide (***R***)-**76** (36 mg, 71% yield) as colorless sticky oil. ^{1}H NMR (400 MHz, $CDCl_3$) δ 8.68 (t, J = 5.60 Hz, 1H), 8.61 (m, 2H), 8.56 (dd, J = 0.80, 4.00 Hz, 1H), 7.93 (s, 1H), 7.85 (m, 2H), 7.75 (d, J = 9.20 Hz, 1H), 7.64 (dt, J = 1.60, 7.60 Hz, 1H), 7.38 (m, 2H), 7.23 (d, J = 8.00 Hz, 1H), 7.17 (dd, J = 5.00, 7.40 Hz, 1H), 4.11 (m, 1H), 3.97 (m, 2H), 3.18 (t, J = 6.20 Hz, 3H), 1.85 (m, 1H), 1.26 (d, J = 6.40 Hz, 3H), 0.99 (d, J = 6.40 Hz, 3H), 0.98 (d, J = 6.80 Hz, 3H).

4.1.6. 4-(1-Methyl-1*H*-indol-2-yl)pyridine-2,6-dicarboxylic acid dimethyl ester (5)

A mixture of 4-bromopyridine-2,6-dicarboxylic acid dimethyl ester (548 mg, 2.00 mmol), 1-methylindole-2-boronic acid (402 mg, 2.30 mmol), sodium bicarbonate (342 mg, 4.07 mmol), and tetrakis(triphenylphosphine)palladium (68 mg, 0.08 mmol) was placed in a 100 mL-flask and dried under vacuum for 2.5 h. In a separate flask, a mixture of toluene (30 mL), methanol (7.5 mL) and water (7.5 mL) was degassed by bubbling argon gas for 2.5 h. The degassed solvent mixture was added to the dried reagents and the combined ingredients were stirred under argon atmosphere at 70 °C. After stirring for 19 h, the mixture was cooled to room temperature, diluted with dichloromethane, washed with brine and dried over sodium sulfate. After rotary evaporation, the residue was purified using silica gel chromatography (40% ethyl acetate in hexanes) to provide **5** (420 mg, 59% yield) as a light yellow solid. ^{1}H NMR (400 MHz, $CDCl_3$) δ 8.47 (s, 2H), 7.69 (td, J = 1.00, 7.60 Hz, 1H), 7.42 (dd, J = 0.80, 8.40 Hz, 1H), 7.35 (dt, J = 1.20, 8.40 Hz, 1H), 7.20 (ddd, J = 1.20, 7.20, 8.00 Hz, 1H), 6.91 (d, J = 0.80 Hz, 1H), 4.07 (s, 6H), 3.88 (s, 3H). ^{13}C NMR (101 MHz, $CDCl_3$) δ 165.26, 148.76, 143.28, 139.89, 136.60, 127.66, 127.00, 123.88, 121.62, 120.86, 110.23, 105.73, 53.54, 31.97.

4.1.7. 4-(1-Methyl-1*H*-indol-2-yl)pyridine-2,6-dicarboxylic acid (6)

To a suspension of dimethyl ester **5** (418 mg, 1.28 mmol) in methanol (15 mL) and tetrahydrofuran (5 mL) was added 1 N aqueous sodium hydroxide (4 mL) and the mixture was stirred at room temperature for 68 h. The reaction was quenched with 1 N aqueous hydrochloric acid (4 mL) with ice-cooling and the mixture was evaporated to dryness. The residue was suspended with methanol–tetrahydrofuran (v/v = 3:1, 40 mL) and filtered through a pad of diatomaceous earth. The filtrate was evaporated dryness, suspended with methanol, and filtered through a pad of diatomaceous earth. Evaporation of the solvents afforded diacid **6** (387 mg, quantitative) as an orange solid, which was used for the next step without further purification. ^{1}H NMR (400 MHz, DMSO-d_6) δ 8.36 (s, 2H), 7.65 (d, J = 7.60 Hz, 1H), 7.57 (dd, J = 2.00, 8.40 Hz, 1H), 7.28 (ddd, J = 1.20, 7.20, 8.40 Hz, 1H), 7.13 (ddd, J = 0.80, 7.20, 8.00 Hz, 1H), 7.00 (d, J = 0.80 Hz, 1H), 3.86 (s, 3H).

4.1.8. (*R*)-4-(1-Methyl-1*H*-indol-2-yl)-N^2-(3-methylbutan-2-yl)-N^6-(2-(pyridin-2-yl)ethyl)pyridine-2,6-dicarboxamide ((*R*)-84)

A mixture of compound **6** (85 mg, 0.25 mmol), 1-hydroxybenzotriazole (83 mg, 0.61 mmol) and 1-ethyl-3-dimethylaminopropylcarbodiimide hydrochloride (EDCI, 105 mg, 0.55 mmol) in DMF (4 mL) was stirred at room temperature for 2.5 h. A mixture of 2-(2-aminoethyl)pyridine (30 mg, 0.25 mmol) and (*R*)-3-methyl-2-butylamine (33 mg, 0.38 mmol) in DMF (1 mL) was added with ice-cooling and the whole was stirred with ice-cooling for 1 h then at room temperature. After stirring for 4 days, the mixture evaporated to dryness and the residue was chromatographed on silica gel to afford (***R***)-**84** (46 mg, 39% yield). ^{1}H NMR (400 MHz, $CDCl_3$) δ 8.67 (br t, J = 5.60 Hz, 1H), 8.58 (ddd, J = 0.80, 1.60, 4.80 Hz, 1H), 8.51 (d, J = 1.60 Hz, 1H), 8.50 (d, J = 1.60 Hz, 1H), 7.73 (br d, J = 9.20 Hz, 1H), 7.68 (m, 1H), 7.65 (dt, J = 1.60, 7.60 Hz, 1H), 7.40 (dd, J = 0.80, 8.40 Hz, 1H), 7.32 (ddd, J = 1.20, 7.20, 8.40 Hz, 1H), 7.24 (d, J = 8.00 Hz, 1H), 7.18 (m, 2H), 6.89 (d, J = 0.80 Hz, 1H), 4.11 (m, 1H), 3.98 (m, 2H), 3.86 (s, 3H), 3.18 (t, J = 6.20 Hz, 2H), 1.87 (m, 1H), 1.27 (d, J = 6.80 Hz, 3H), 1.00 (d, J = 6.80 Hz, 3H), 0.99 (d, J = 6.40 Hz, 3H). ESI-MS: m/z $[M+Na]^+$ 492.2, $[M+H]^+$ 470.3.

4.2. Cloning and expression of recombinant human STAT6

Full length human STAT6 gene was cloned into a pBac-based baculovirus transfer vector. Sapphire DNA was used to create recombinant virus for P0. The P0 virus was used to produce P1 and further P2 virus. The P2 virus was used to infect 1 L of Sf21 cells at 1×10^6 cells/ml. Cells were collected three days after infection. Cells were lysed in lysis buffer (1× PBS, pH7.4, 0.4% CHAPS, 0.05% Triton X-100, protease inhibitor tablet EDTA-free from Roche, 10 mM BME). The recombinant STAT6 protein was purified using Ni-NTA beads (Qiagen) to yield 24 mg/L of Sf21 cells. The protein was dialyzed against PBS with 1 mM DTT, 1 mM EDTA, and 10% glycerol, and used for both inhibitor screening and binding characterizations.

For transient expression in mammalian cells, human STAT6 and mouse STAT6 genes were cloned into the pEAK12 vector. The resulting plasmids were used for studies involving 293-EBNA cells and BEAS-2B cells as discussed below.

4.3. Cell based assays

4.3.1. STAT6 reporter assay and eotaxin-3 secretion ELISA assay

The STAT6 reporter construct was created by inserting six copies of IL-4 response element CTTCCCAAGAA into a construct that expresses the *Photinus* luciferase gene.[26] 293-EBNA cells were grown in 96-well plate to 90% confluency. The cells were co-transfected with the STAT6 reporter and human STAT6 using Lipofectamine2000 from Invitrogen. The transfected cells were changed into serum free media after one day of transfection. The cells were incubated with each compound for 1 h and then treated with 10 ng/ml IL-4 or control. After 6 h of induction, the cells were analyzed by luciferase activity using the Promega duo luciferase kit. The experiments were performed in duplicates.

For eotaxin detection, BEAS-2B cells and A549 cells were grown to 90% confluency in DMEM and serum starved for 24 h. Each compound was added to the cells for 1 h, followed by addition of IL-4 to 50 ng/mL concentration. The cells were further incubated for 24 h. The media were collected and the amount of eotaxin-3 measured by ELISA using the Duoset CCL26/eotaxin-3 kit (R&D Systems). The experiments were performed in duplicates.

4.3.2. Immunoassay and immunoprecipitation

N-Terminal HA and myc tagged STAT plasmids were co-transfected into 293-EBNA cells. The cells were serum starved after growing in regular media for one day and treated with inhibitors and IL-4 on the third day. The cells were washed once with PBS and lysed in the lysis buffer (PBS, 0.05% Tween-20, protease inhibitor cocktail EDTA-free). Each resulting lysate sample was

incubated with HA-agarose beads for 1 h, washed with lysis buffer for three times, boiled in sample buffer, and blotted with anti-HA, anti-Myc, anti-STAT6 and anti-phospho-STAT6 antibodies.

4.4. Biochemical assays

4.4.1. STAT6 interaction with IL-4R derived peptides

IL-4 receptor derived peptide GASSGEEGYKPFQDLI was synthesized by Invitrogen. The p-IL-4R peptide is phosphorylated at the tyrosine residue, which is not phosphorylated in the control IL-4R peptide. The peptides were biotinylated at the N-terminus. Reacti-bind™ streptavidin coated 96-well plate was coated with 20 μg/mL of each peptide in PBS. A mixture of each small molecule inhibitor (20 μM) with various concentrations of recombinant STAT6 was added to the plate and incubated at rt for 1 h. The bound STAT6 was detected by anti-STAT6 mouse antibody and anti-mouse HRP conjugate. The experiments were done in duplicates or triplicates.

4.4.2. In vitro JAK2 kinase activity assay

HTScan® JAK2 kinase assay kit (Cell Signaling Technology) was used following the manufacturer's instructions. Additional reagents used in this assay, including Stop solution, TMB solution, and HRP-conjugated anti-mouse IgG antibody, were obtained from Cell Signaling Technology. After incubation at room temperature for 30 min, the reaction mixtures were transferred to a 96-well streptavidin-coated plate (PerkinElmer). JAK2 activity was measured by colorimetric ELISA. The experiments were done in triplicates.

4.4.3. STAT6-inhibitor binding assay using SPR

The experiments were performed on a BIAcore T100, using Sensor Chip CM5 (Series S), amine coupling kit, and PBS buffer from BIAcore.

Immobilization of STAT6 was performed at 25 °C on sensor chip CM5 (series S) in PBS running buffer (20 mM sodium phosphate, 150 mM sodium chloride, pH 7.4), at a flow rate of 10 μL/min. Flow cells were activated for 7 min by injecting a mixture of 50 mM NHS and 200 mM EDC (70 μL). To prepare a high-capacity surface, 70 μL of STAT6 solution (25 μg/mL) in sodium acetate buffer (pH 5.0) was injected for 7 min, followed by injection of 70 μL ethanolamine to block any remaining surface-activated groups. Typical immobilization levels ranged from 12,000 to 14,000 RU. Non-derivatized flow cells served as reference surfaces.

All the assays were performed at 25 °C on the sensor chip described above. All compounds were stored as 10 mM stock solutions in dimethyl sulfoxide (DMSO). After dilution to 2 mM with DMSO, each sample was mixed with 1.05-fold concentrated assay buffer and DMSO to yield a 100 μM compound solution in pH 7.4 buffer with a final composition of 20 mM sodium phosphate, 150 mM sodium chloride, and 5% DMSO, which was also used as the instrument running buffer and sample dilution buffer. All assays were run at a flow rate of 30 μL/min and a data collection rate of 10 Hz. Each run was started with five start-up cycles in which running buffer was injected instead of sample, followed by sample injection cycles. A duplicate sample and a zero concentration sample were used as a positive and negative control. A typical analysis cycle consisted of a 60 s sample injection, 600 s of buffer flow (dissociation phase), followed by a wash with 25% DMSO and buffer, and finally a 30 s buffer injection to check for sample carryover. Between sample series, several solvent correction cycles were run to adjust for referencing errors due to refractive index mismatches between running buffer and samples.

Calculated equilibrium dissociation constants (K_D), association rate (k_a), and dissociation rate (k_d) were obtained by global fitting of SPR sensorgrams to a 1:1 Langmuir binding model. The χ^2 value represents the sum of squared differences between the experimental data and reference data at each point of the fit.

Acknowledgments

We thank our colleagues at NeoGenesis and MGH for performing the initial in vitro screening for the STAT6 binders and providing related results and procedures.

References and notes

1. Kasaian, M. T.; Miller, D. K. *Biochem. Pharmacol.* **2008**, *76*, 147.
2. Foster, P. S.; Martinez-Moczygemba, M.; Huston, D. P.; Corry, D. B. *Pharmacol. Ther.* **2002**, *94*, 253.
3. Akimoto, T.; Numata, F.; Tamura, M.; Takata, Y.; Higashida, N.; Takashi, T.; Takeda, K.; Akira, S. *J. Exp. Med.* **1998**, *187*, 1537.
4. Kuperman, D.; Schofield, B.; Wills-Karp, M.; Grusby, M. J. *J. Exp. Med.* **1998**, *187*, 939.
5. Kuperman, D. A.; Huang, X.; Koth, L. L.; Chang, G. H.; Dolganov, G. M.; Zhu, Z.; Elias, J. A.; Sheppard, D.; Erle, D. J. *Nat. Med.* **2002**, *8*, 885.
6. Rawlings, J. S.; Rosler, K. M.; Harrison, D. A. *J. Cell Sci.* **2004**, *117*, 1281.
7. Shuai, K.; Horvath, C. M.; Huang, L. H.; Qureshi, S. A.; Cowburn, D.; Darnell, J. E., Jr. *Cell* **1994**, *76*, 821.
8. Ota, N.; Brett, T. J.; Murphy, T. L.; Fremont, D. H.; Murphy, K. M. *Nat. Immunol.* **2004**, *5*, 208.
9. Braunstein, J.; Brutsaert, S.; Olson, R.; Schindler, C. *J. Biol. Chem.* **2003**, *278*, 34133.
10. Mao, X.; Ren, Z.; Parker, G. N.; Sondermann, H.; Pastorello, M. A.; Wang, W.; McMurray, J. S.; Demeler, B.; Darnell, J. E., Jr.; Chen, X. *Mol. Cell* **2005**, *17*, 761.
11. Zhong, M.; Henriksen, M. A.; Takeuchi, K.; Schaefer, O.; Liu, B.; ten Hoeve, J.; Ren, Z.; Mao, X.; Chen, X.; Shuai, K.; Darnell, J. E., Jr. *Proc. Natl. Acad. Sci. U.S.A.* **2005**, *102*, 3966.
12. Wenta, N.; Strauss, H.; Meyer, S.; Vinkemeier, U. *Proc. Natl. Acad. Sci. U.S.A.* **2008**, *105*, 9238.
13. Schust, J.; Sperl, B.; Hollis, A.; Mayer, T. U.; Berg, T. *Chem. Biol.* **2006**, *13*, 1235.
14. Siddiquee, K.; Zhang, S.; Guida, W. C.; Blaskovich, M. A.; Greedy, B.; Lawrence, H. R.; Yip, M. L.; Jove, R.; McLaughlin, M. M.; Lawrence, N. J.; Sebti, S. M.; Turkson, J. *Proc. Natl. Acad. Sci. U.S.A.* **2007**, *104*, 7391.
15. Turkson, J.; Kim, J. S.; Zhang, S.; Yuan, J.; Huang, M.; Glenn, M.; Haura, E.; Sebti, S.; Hamilton, A. D.; Jove, R. *Mol. Cancer Ther.* **2004**, *3*, 261.
16. Gunning, P. T.; Katt, W. P.; Glenn, M.; Siddiquee, K.; Kim, J. S.; Jove, R.; Sebti, S. M.; Turkson, J.; Hamilton, A. D. *Bioorg. Med. Chem. Lett.* **2007**, *17*, 1875.
17. Duan, Z.; Bradner, J. E.; Greenberg, E.; Levine, R.; Foster, R.; Mahoney, J.; Seiden, M. V. *Clin. Cancer Res.* **2006**, *12*, 6844.
18. McCusker, C. T.; Wang, Y.; Shan, J.; Kinyanjui, M. W.; Villeneuve, A.; Michael, H.; Fixman, E. D. *J. Immunol.* **2007**, *179*, 2556.
19. Chiba, Y.; Todoroki, M.; Nishida, Y.; Tanabe, M.; Misawa, M. *Am. J. Respir. Cell Mol. Biol.* **2009**, *12*, 23.
20. Nagashima, S.; Nagata, H.; Iwata, M.; Yokota, M.; Moritomo, H.; Orita, M.; Kuromitsu, S.; Koakutsu, A.; Ohga, K.; Takeuchi, M.; Ohta, M.; Tsukamoto, S. *Bioorg. Med. Chem.* **2008**, *16*, 6509.
21. Nagashima, S.; Yokota, M.; Nakai, E.; Kuromitsu, S.; Ohga, K.; Takeuchi, M.; Tsukamoto, S.; Ohta, M. *Bioorg. Med. Chem.* **2007**, *15*, 1044.
22. Sakurai, M.; Nishio, M.; Yamamoto, K.; Okuda, T.; Kawano, K.; Ohnuki, T. *J. Antibiot.* **2003**, *56*, 513.
23. Annis, D. A.; Nickbarg, E.; Yang, X.; Ziebell, M. R.; Whitehurst, C. E. *Curr. Opin. Chem. Biol.* **2007**, *11*, 518.
24. Annis, D. A.; Cheng, C. C.; Chuang, C. C.; McCarter, J. D.; Nash, H. M.; Nazef, N.; Rowe, T.; Kurzeja, R. J.; Shipps, G. W., Jr. *Comb. Chem. High Throughput Screen.* **2009**, *12*, 23.
25. Whitehurst, C. E.; Annis, D. A. *Comb. Chem. High Throughput Screen.* **2008**, *11*, 427.
26. Pesu, M.; Aittomaki, S.; Valineva, T.; Silvennoinen, O. *Eur. J. Immunol.* **2003**, *33*, 1727.
27. Yoshida, I.; Suzuki, S. US Patent 7,217,723, 2007.
28. Matsukura, S.; Stellato, C.; Georas, S. N.; Casolaro, V.; Plitt, J. R.; Miura, K.; Kurosawa, S.; Schindler, U.; Schleimer, R. P. *Am. J. Respir. Cell Mol. Biol.* **2001**, *24*, 755.
29. Kagami, S.; Saeki, H.; Komine, M.; Kakinuma, T.; Tsunemi, Y.; Nakamura, K.; Sasaki, K.; Asahina, A.; Tamaki, K. *Clin. Exp. Immunol.* **2005**, *141*, 459.
30. Blanchard, C.; Durual, S.; Estienne, M.; Emami, S.; Vasseur, S.; Cuber, J. C. *Int. J. Biochem. Cell Biol.* **2005**, *37*, 2559.
31. Hoeck, J.; Woisetschlager, M. *J. Immunol.* **2001**, *167*, 3216.
32. Hoshino, A.; Tsuji, T.; Matsuzaki, J.; Jinushi, T.; Ashino, S.; Teramura, T.; Chamoto, K.; Tanaka, Y.; Asakura, Y.; Sakurai, T.; Mita, Y.; Takaoka, A.; Nakaike, S.; Takeshima, T.; Ikeda, H.; Nishimura, T. *Int. Immunol.* **2004**, *16*, 1497.
33. Nishimura, Y.; Nitto, T.; Inoue, T.; Node, K. *Circ. J.* **2008**, *72*, 469.
34. Stolzenberger, S.; Haake, M.; Duschl, A. *Eur. J. Biochem. FEBS* **2001**, *268*, 4809.
35. Mertens, C.; Zhong, M.; Krishnaraj, R.; Zou, W.; Chen, X.; Darnell, J. E. *Genes Dev.* **2006**, *20*, 3372.
36. Choi, J. H.; Banks, A. S.; Kamenecka, T. M.; Busby, S. A.; Chalmers, M. J.; Kumar, N.; Kuruvilla, D. S.; Shin, Y.; He, Y.; Bruning, J. B.; Marciano, D. P.; Cameron, M. D.; Laznik, D.; Jurczak, M. J.; Schürer, S. C.; Vidović, D.; Shulman, G. I.; Spiegelman, B. M.; Griffin, P. R. *Nature* **2011**, *477*, 477.